

Fish otolith trace element maps: new approaches with synchrotron microbeam x-ray fluorescence

Karin E. Limburg,^{1*} Rong Huang² and Donald H. Bilderback³

¹ SUNY College of Environmental Science and Forestry, Syracuse, NY 13210, USA

² IMCA-CAT, Center for Advanced Radiation Source, University of Chicago, Chicago, IL 60637, USA

³ Cornell High Energy Synchrotron Source and School of Applied and Engineering Physics, Cornell University, Ithaca, NY 14853, USA

Received 29 September 2006; Revised 16 April 2007; Accepted 16 May 2007

Otoliths, the carbonate earstones of fishes, take up minor and trace amounts of elements as they accrete through a fish's life. We apply synchrotron microbeam x-ray fluorescence methods to establish a breakthrough in high-resolution, simultaneous area mapping of multiple trace elements in otoliths, with spatial resolution down to 20 μm and trace element detection down into the part per million range for multiple elements. Concentration maps of Ca, Sr, Zn and, for the first time, Ba, Mn, and Se are obtained simultaneously. Combinations of these elemental maps provide new insights into the environmental history of fishes and their lifetime movements, illustrated by several case studies. This method helps pave the way toward improved spatial analysis of otolith microchemistry. Copyright © 2007 John Wiley & Sons, Ltd.

INTRODUCTION

A virtual revolution in fisheries biology and ecology has been driven by otolith analysis. These small (generally <20 mm), calcareous concretions form part of the hearing and balance system in bony fishes and are located underneath the braincase. Otoliths grow incrementally, and these increments can be resolved at both daily and annual time scales.¹ Optical examination of macro- and micro-increments for age and growth determination is now the standard in many labs around the world, with over a million otoliths annually examined.¹

Microchemical analysis of otoliths constitutes a second revolution currently under way, with new discoveries and applications. Over 30 elements have been identified in otoliths, most of them in trace amounts.² Among these, strontium has been one of the most reliable minor elements to quantify; transects of Sr:Ca ratios, measured from the core to the outer edge of otoliths, have been widely used to reconstruct the histories of movements in and out of different ecosystems.^{3–5} However, accurate quantification of true trace elements has been problematic, owing to a number of issues including matrix effects,⁶ contamination or loss of elements upon handling,^{7–9} and detection limits. Currently, most trace elemental analysis is conducted with wet chemistry methods (e.g. inductively coupled plasma mass spectrometry ICPMS) or with laser ablation (LA) ICPMS. Although able to detect concentrations down to parts per billion, both of these methods destroy the sample and explore limited areas of the otolith. Nondestructive, high-resolution methods that sample the entire surface would be preferable. Furthermore, although fine-scale sampling is possible with LA-ICPMS, in

general only a small part of an otolith is assayed, e.g. the core.

Line transect analyses from the otolith core to the outer edge produce a record of the elemental variation throughout the life of a fish; most transects have been established for strontium and a few other minor elements (e.g. Na, Mg, and K).² However, creating full-area 2D maps of elemental concentrations reveals their true heterogeneity in otoliths, and in many ways is preferable to a single point sample or line transect. Maps are acquired nondestructively using x-ray fluorescence spectrometry. A capillary that produces a 20 micron spot provides a resolution of 1270 dpi, which brings out details easily discernible to the human eye. Electron microprobes have micron-scale mapping capability but are generally limited to concentrations in the parts-per-thousand range. Nuclear microscopy with proton-induced x-ray emission (μPIXE) analysis can achieve parts-per-million detection at the micron scale, but the presence of significant amounts of sodium in otoliths generates gamma reactions that swamp out the signals of many trace elements.⁶

Recently we have begun experiments that apply x-ray microbeam techniques to the problem of mapping trace elemental variations in otoliths with synchrotron x-ray fluorescence (XRF) methods. Our results show that nondestructive area (several millimeters) maps of the trace element distributions are feasible and that approximate elemental concentrations can be determined, some of them for the first time. Thus this method presents an alternative to the destructive methods used for measuring trace elements in otoliths. The development of multiple maps of different trace elements greatly enhances the information obtained about past environments experienced by individual fish. Below we discuss the x-ray microbeam technique, sample preparation, concentrations determined by simulation, and results from several case studies. We conclude that although more studies

*Correspondence to: Karin E. Limburg, Faculty of Environmental and Forest Biology, SUNY College of Environmental Science and Forestry, Syracuse, NY 13210, USA. E-mail: KLimburg@esf.edu

are needed, new and novel environmental information about the life history of a particular fish can be obtained even from our preliminary findings.

MATERIALS AND METHODS

X-ray microbeam technique and sample preparation

Mapping otolith trace elements with XRF requires a small microbeam with high x-ray flux for good spatial resolution and low detection capability. Three types of glass capillary optics are typically used on synchrotron sources for this kind of microbeam work: polycapillaries, single-bounce monocapillaries, and multi-bounce monocapillaries.^{10–12} For our experiments we used single-bounce monocapillaries made at the Cornell High Energy Synchrotron Source (CHESS).^{13,14} Depending on the design, these capillaries can focus x-rays into 12–20 μm spot sizes at CHESS, with 30 to 55 mm working distances (the distance from the capillary tip exit to the sample position) and an increase of the x-ray flux density of up to more than 400 times at the focusing point. X-rays were obtained at the CHESS D-line bending magnet source downstream of a 1% bandwidth multilayer monochromator. We have measured a flux of up to 1.0×10^{12} photons/s from a single-bounce capillary producing a 20- μm focal spot with 8 mrad of divergence at 10 keV during operation of the storage ring (5.3 GeV and 125 mA). An XFlash detector (Röntec) was used to detect the x-ray fluorescence from the otolith. A layer of 38 μm 99.999% pure aluminum foil was routinely used, to attenuate the otolith's large Ca fluorescence, in front of the detector to increase the sensitivity for trace elements. Occasionally, an 8- μm thick foil of 99.9% pure Co was added to reduce detector background and to increase the detecting sensitivity of Ba L lines (from 4.47 to 5.16 keV) by absorbing otolith scattering from the incident x-rays (8 keV in this instance). The x-ray fluorescence collected by the detector after filtering was still in the range of 30 000 to 100 000 counts per second (cps), because of the use of the capillary. With the XFlash detector, the fluorescence spectrum of multiple trace elements was recorded for 6–11 s per pixel. This made it possible to raster-scan an entire otolith in several hours, although more than 24 h was required in some extreme cases. Both the step size and the number of pixels per image varied according to the size and type of the otolith. For example, there were 40 to 110 steps in the *x*- or *y*-direction of the otoliths studied in this paper, with step size ranging from 25 μm (in both dimensions of Fig. 3) to 120 μm (in the horizontal dimension of the 12 mm long otolith in Fig. 4). By recording the XRF spectrum at each position we mapped out several elements simultaneously including major (Ca), minor (Sr), and trace constituents (Ba, Mn, Zn, Se, Rb, Cu, etc.). MATLAB software (The MathWorks, Inc.) was used to visualize the data.

To prepare the samples, otoliths were embedded in clean epoxy, sectioned, ground to the appropriate thickness (50–100 μm), mounted on Suprasil silicate slides (Heraeus Quartz America), and ultrasonicated in deionized (18 M Ω) water. Care was taken to minimize contamination of both the top and bottom surfaces of the otolith specimens; this is because the x-rays penetrate the entire thin section

and interact with materials beneath it. The ultrapure glass slides facilitated preparation (by stabilizing the otolith while grinding and polishing) and did not interfere with the analyses. The x-ray detector was positioned at 90° to the capillary axis to minimize scattering from the sample (Fig. 1). The sample face was placed at the capillary focal position at 45° to both the capillary and the detector axes. The incident x-ray energy from the multilayer monochromator was set between 8 and 10 keV to excite the fluorescence of such elements as Ca, Fe, Mn, and Zn, with the second harmonic (between 16 and 20 keV) used to excite heavier elements such as Sr and Se. The typical second harmonic intensity at 18 keV was about 1.7% of the fundamental intensity at 9 keV.

Determining elemental concentrations

Because we lacked an appropriate otolith standard, a well-established XRF simulation code¹⁵ based on Monte Carlo methods and the 'variance reduction technique' was used to estimate trace element concentrations and detection limits. This simulation code developed by L. Vincze *et al.* is a very comprehensive one including not only all the atomic processes but also the experimental setups such as sample substrates, surrounding air pass, filters, detector response functions. The x-ray atom interactions, where the matrix effect comes from, can be simulated up to ten times of collisions for each x-ray before it is detected or escaped away. The average error of simulated concentrations was only 3–6% in the case of biological materials and a standard sample is not needed.¹⁵ In our otolith case, the situation is even simpler because the major components of an otolith are already known and what needs to be determined is only those trace elements mostly in ppm concentration ranges with relatively weaker inter-element corrections. Since the primary purpose of the XRF measurement is the determination of fish life histories rather than demonstrating the ultimate accuracy of trace element measurement, several assumptions were used to simplify the simulation models. The otolith density was assumed to be the same as stoichiometric CaCO₃ (1.55 g/cm³), with 40% Ca by weight.

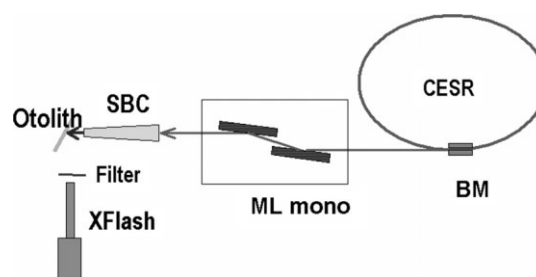


Figure 1. Schematic of otolith XRF experiment. X-rays out of a bending magnet (BM) of the Cornell Electron Storage Ring (CESR) were monochromatized by a 1% energy bandwidth multilayer monochromator (ML mono), and then were focused by a single-bounce capillary (SBC) to an otolith sample with focal size of 20 μm (28 μm footprint in the horizontal direction of the 45° tilted sample). An XFlash energy dispersive detector was used to collect the XRF spectrum from the sample. A 2D scan stage underneath the sample moved the sample to make the XRF images.

The very thin boundary layer between the otolith and the Suprasil slide was neglected in the simulation. The slide was assumed to be pure SiO₂, and the appearance of other trace elements inside the slide was assumed to be negligible (later confirmed by a separate XRF test). The sample and its trace element distributions were assumed to be uniform within the resolution volume, which is a reasonable simplification as long as the spatial variation of elemental concentrations is on a larger scale than the experimental resolution. The simulation solves for trace element concentrations on the basis of the assumed 40% Ca concentration and the measured trace element intensities relative to Ca. Trace element minimum detectable limit was estimated as 3 times the square root of the fluorescence background counts. For the cases where Sr was excited by the second-harmonic x-rays from the multilayer monochromator, the x-ray relative intensity of the second to the first harmonic was simulated from measuring otolith scattering intensities of both harmonics. We also learned from the XRF simulations that when sample thickness changes from 50 to 100 µm, the element intensities (from Ca, Ba, Mn, Zn) excited by 9.8 keV x-rays will not change by more than 15%, and the relative intensities (from Se, Sr) to Ca intensities excited by 19.6 keV second harmonic x-rays will increase only by 30–45%. The ratio of first to second harmonic x-ray scattering changes no more than 12% when sample thickness changes from 50 to 100 µm. These results indicate that the detected XRF maps reveal mainly the concentration distribution and are not sensitive to small variations of the sample thickness, which are expected to vary slowly over the length scale of a few millimeters. In summary, our XRF simulations suggest elemental concentration accuracies of better than a factor of 2 for our simplified model.

ASSESSMENT

Case studies: reconstructing fish histories through combined minor and trace elements

As illustrated below in several case studies, we applied this microbeam x-ray technique to map several trace elements in otoliths from both anadromous (migrating between marine and fresh water) and freshwater fishes. We then show the utility of the maps to help unravel the past environmental histories of individual fish.

Case study 1: Baltic Sea whitefish (Salmonidae: *Coregonus lavaretus*)

Once a common species in the Baltic Sea, whitefish is among a class of fishes in decline along the Swedish east and southeast coasts.¹⁶ Brackish water residents and anadromous forms coexist around the central Baltic island of Gotland, Sweden, but the relative proportions are in question. Previous elemental mapping with µPIXE (K. E. Limburg and M. Elfman, unpublished data) had revealed patterns of Sr:Ca consistent with both anadromy and marine residency. We selected an otolith from an anadromous individual for the first monocapillary experiment. The images of Ca, Sr, Zn, and Mn were easily mapped with XRF, Fig. 2.

The Ba L line peaks were very weak, and barely distinguishable from the detector background and other

random peaks possibly owing to very small amounts of sample surface contaminants due to sample preparation. Nevertheless we could detect Ba by fitting a spectrum to standard Ba L line XRF peaks, avoiding false counting of contaminants (Fig. 2(D)). Better detection was also gained by use of an additional Co filter to reduce scattering of x-rays into the detector. Because of Baltic drainage basin geology,^{17–19} we expected that barium concentrations would be inversely related to strontium, and so postulated that Ba, a trace element, would be detected in the Sr-depleted part of the otolith. Strontium was depleted in the interior of the otolith, and as predicted, this zone was enriched in Ba (Fig. 2(C) and (D)). This zone corresponds to the period of freshwater residency for the fish, and the Sr pattern is similar to that of anadromous brown trout.²⁰ Zinc and manganese were also detectable (Fig. 2(E) and (F)). Zinc intensity peaked in annual growth rings, which has been detected in other members of the salmon family.^{20,21} Manganese patterns (Fig. 2(F)) were completely different from the other elements and probably indicate movements between different habitats even within the brackish sea, perhaps reflecting Mn availability from variable redox conditions. The Mn and Ba absolute concentrations are in the parts-per-million range, while the Sr is in the parts-per-thousand range.

Case study 2: blueback herring (Clupeidae: *Alosa aestivalis*)

Blueback herring is another anadromous fish, but native to eastern North America.²² The subfamily to which it belongs includes many species that move between marine and fresh water, and some, like the alewife (*A. pseudoharengus*), establish inland populations (Laurentian Great Lakes). Both species are native to the Hudson River estuary, defined as the 252-km tidal stretch between New York City and the Federal dam at Troy, NY. However, over the past 70 years blueback herring gradually expanded their range into the Mohawk River, a major westward tributary that became accessible only when navigation locks were constructed.²³ The Mohawk is part of the New York State Barge Canal system with connecting canals, lakes, and rivers ultimately draining into both Lakes Ontario and Erie. The 1994 finding of thousands of blueback herring in the Oswego River near Lake Ontario, followed by two juveniles in the lake itself in 1995,²³ spurred concern about the potential for the species to become a new Great Lakes invader.

Adults collected in the Mohawk River in 1999 for otolith analysis had surprisingly variable levels of Sr:Ca.²⁴ Resident juveniles in the Mohawk River had higher Sr:Ca than juveniles in the Hudson River downstream; hence, an upriver source or sources of Sr was suspected. Subsequent water sampling in 2001 and 2002 located several sources of elevated Sr:Ca, primarily in Oneida Lake and its southern tributaries.²⁵ In addition, manganese and barium varied geographically; the combination of relative levels of Sr:Ca, Mn:Ca, and Ba:Ca could identify spatially discrete zones. In particular, Mn:Ca is at a maximum, Sr:Ca a minimum, and Ba:Ca relatively elevated in the headwaters region of the Mohawk River at Rome, NY. Sr:Ca and Mn:Ca are low in the tidal Hudson, whereas Ba:Ca is moderately high; and

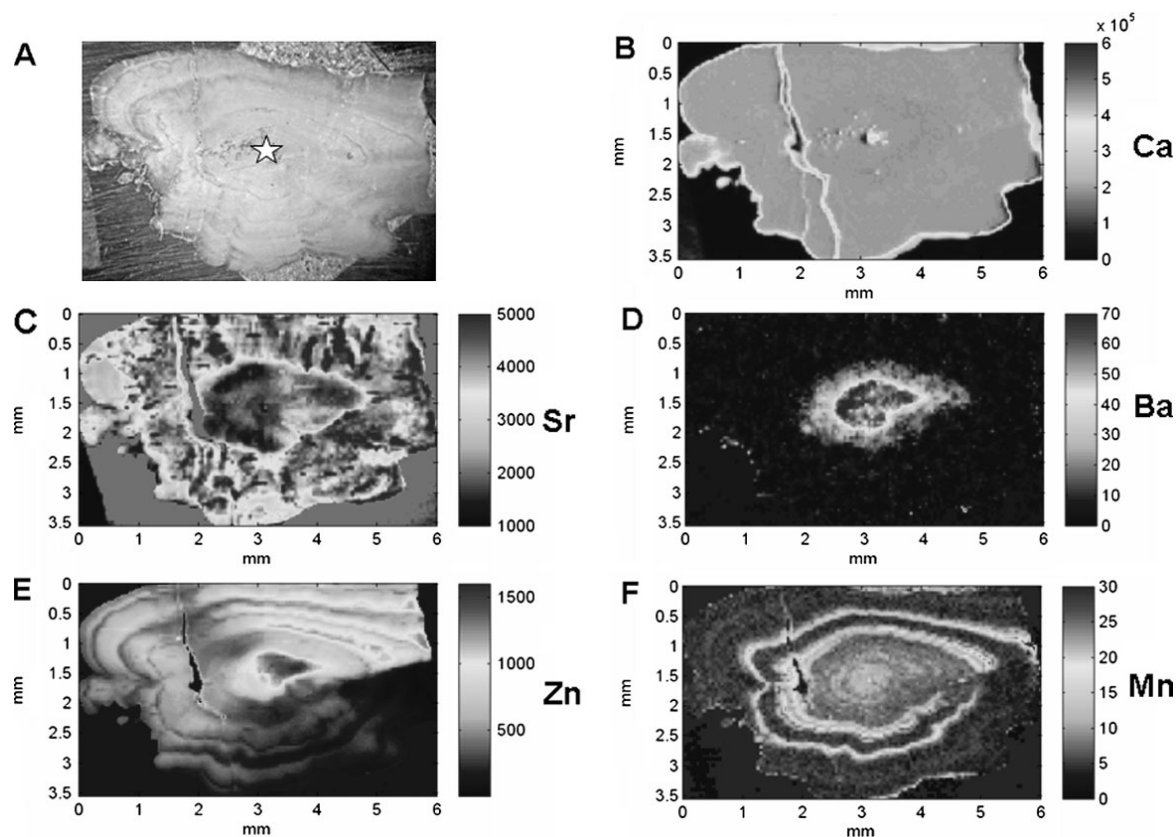


Figure 2. Optical image (A) and elemental maps (simultaneously collected) of (B) calcium, (C) strontium, (D) barium, (E) zinc, and (F) manganese in a whitefish *Coregonus lavaretus* otolith; core is marked with a star. Dorsal side is facing down, and the posterior end is to the left. The rostral end (right) was broken off and the posterior was cracked to provide a flatter surface for analysis. The intensity unit of Ca image is in XRF counts and it is very uniform. The unit of other image intensities is ppm, based on XRF simulation described in text. While Sr and Zn concentration are in the parts-per-thousand ranges (average Sr concentration over whole sample is 3600 ppm), Ba and Mn concentrations are in the ppm ranges (Ba and Mn averages over whole sample are 7.4 ppm and 7.2 ppm respectively).

finally, Sr:Ca and Ba:Ca are elevated in Oneida Lake and westward.

We used monocapillary focused microbeam XRF on otoliths from two blueback herrings that were collected from the Mohawk River and that had displayed ambiguous Sr:Ca traces in previous analyses. In both cases, Sr minima co-occurred on the otolith with Mn maxima (Fig. 3(C) and (D)).

Ba is present only in the interior, in the part of the otolith corresponding to the first season's growth (Fig. 3(E)). A high-intensity zone (in red) of Sr corresponds with low Mn and Ba, an elemental signature consistent with marine water. The three tracers together confirm that the fish began life in the Mohawk River, emigrated through the Hudson, and spent at least one winter out at sea. However, elevated Mn in the following year suggests a directed movement to a different location, perhaps the lower estuary.

Case Study 3: fish from a polluted urban lake

Onondaga Lake, along which the city of Syracuse, NY, is established, has a century-long history of abuse and neglect.²⁶ A lake with salt springs, it became a 19th century center for trade and industry as Syracuse profited from its central location on the Erie Canal. Industry and sewage were already a concern before World War I, and a chemical industry

(Solvay, later Allied Chemical) developed on the western shore. Its products included chlorine and NaOH through a chlor-alkali process that involved the use of mercury as an intermediary reductant. Wastes were disposed of directly into the lake or in shoreline waste beds. In all, an estimated 76 metric tons of mercury were discharged into Onondaga Lake from 1946–1970.²⁶ Today the lake remains a Superfund site, with highly elevated, albeit varying, sediment concentrations of mercury as well as other heavy metals. Virtually all resident fish contain measurable amounts of mercury, which bioaccumulates through the food web.

Mercury has been a difficult element to quantify in otoliths,^{2,27,28} with experimental manipulations producing complex results. We hoped mercury, if detectable by our monocapillary XRF method, would show a pattern of accumulation consistent with the history of residency of wild fishes in Onondaga Lake. No Hg XRF has been found from our otolith samples so far, with the estimated Hg detection limit as low as 0.6–1 ppm calculated from the sample XRF spectrum background measurement and XRF simulations. However, unexpectedly, the experiment revealed the presence of selenium in the otoliths from two species examined thus far (a 19-year-old channel catfish (*Ictaluridae: Ictalurus punctatus*) and an 11-year-old

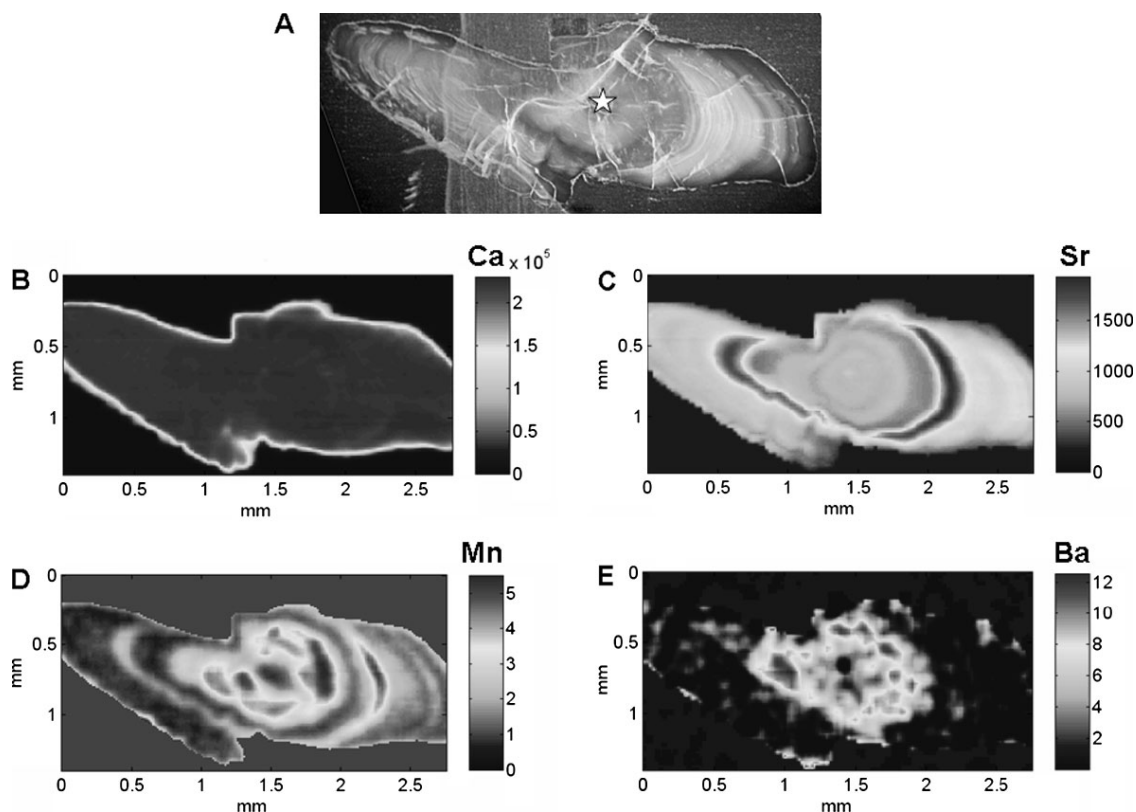


Figure 3. Optical image (A) and calcium (B), strontium (C), manganese (D), and barium (E) maps of an otolith from a blueback herring captured in the Mohawk River at Rome, NY. Otolith core in (A) is marked with a star. Units are as in Fig. 2.

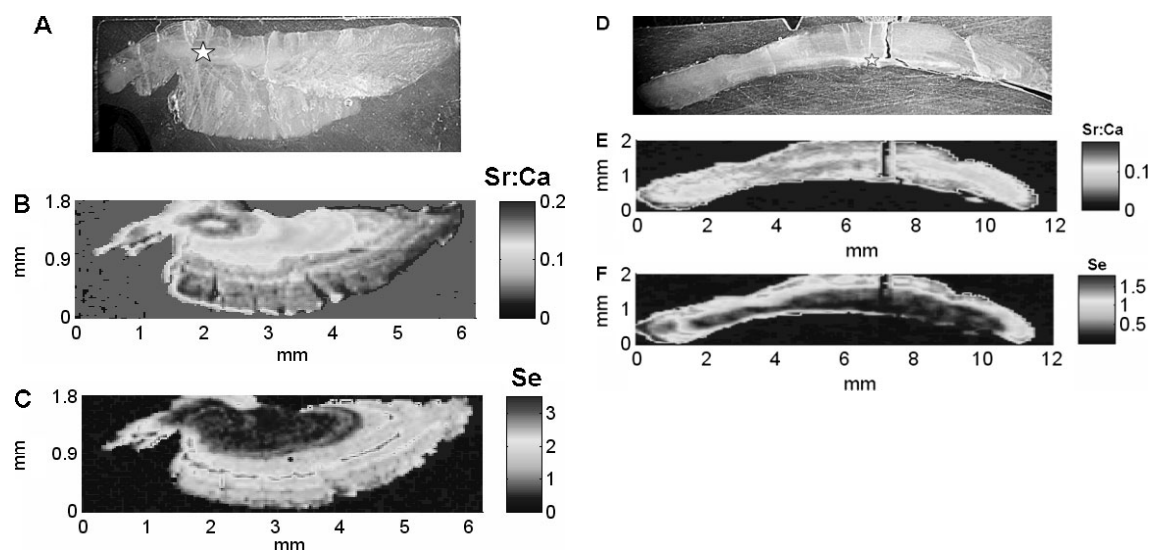


Figure 4. Optical images and elemental maps of strontium (as Sr:Ca) and selenium in transverse sections of otoliths of fish from a polluted urban lake, Onondaga Lake, NY. Stars on the optical images show location of otolith cores. (A–C) Channel catfish, *Ictalurus punctatus* (age determined by counting visible annuli = 19 years). (D–F) Walleye, *Sander vitreum* (age = 11 years). In both couplets, strontium is shown in the top map. Red = highest concentration, dark blue = lowest, with scale of part per million for Se maps and XRF intensity ratio to Ca for Sr maps.

walleye (Percidae: *Zander vitreum*), Fig. 4), with average concentrations about 1 ppm.

Rarely reported as a constituent of otoliths, Se accumulation clearly varied temporally and was not present in the inner parts of the otoliths, indicating that uptake did not begin at birth, but rather after several years of growth (Fig. 4(C) and (F)). Strontium uptake also varied, but in the

catfish otolith (Fig. 4(B)) there were two periods of elevated Sr, separated by a period of lower Sr uptake. Our interpretation of the patterns of Sr and Se in this otolith are that the channel catfish was born in a strontium-rich environment, moved into a Sr-depleted habitat after 2 years, and finally, at 10 years of age, into Onondaga Lake that was enriched in both Sr and Se. The Sr-rich natal habitat could be a nearby

lake with confirmed elevated levels of Sr.²⁵ The concordance of Sr and Se in the walleye otolith (Fig. 4(E) and (F)) is not as clear, because of the narrowness of the cross section, but Sr also appears to be lower in the core. Both fish thus appear to have been born elsewhere, and to have migrated into Onondaga Lake as adults.

Although listed as an element of concern in Onondaga Lake, the presence of Se in both fish's otoliths was unexpected because most of the lake remediation and monitoring studies do not report it, focusing rather on Hg. Selenium is an essential trace element for fish,^{29,30} but is also a known environmental hazard causing birth defects and extirpation of fish and wildlife.^{31,32} Selenium can also moderate the adverse effects of mercury through antagonism, but can also have synergistic effects.^{33,34} Very little is known at this point about the effects of Se on biota in Onondaga Lake, but the fact that it can accumulate in otoliths, and be mapped temporally, demonstrates its potential utility as a marker of contaminant exposure history in individual fish.

DISCUSSION

We have been able to make simultaneous two-dimensional maps of elements such as Ca, Sr, Ba, Cu, Se, Mn, Zn, etc., at concentrations as low as a few parts per million within the otoliths we examined. To our knowledge, this capability has not been previously achieved, although Tsukamoto and colleagues published one of the first reports of Sr analysis using synchrotron XRF.³⁵ Since the incorporation of trace elements depends to large extent on the composition of the local water in which the fish exists (but see caveats^{2,36}), we obtain a time/history view of the environments experienced by the fish. Given enough information about the ratios of trace elements in local regions of a water body, for instance, it may be possible to say how long a fish remained in certain areas by correlating ratios of several trace elements in otoliths with similar ratios as they vary spatially. Indeed, matching otolith chemistry with water chemistry is the basis for at least some stock identification exercises^{37,38} and for identifying nursery habitat,³⁹ in which the chemistry of whole (larval, juvenile) or partial (interior areas in adult) otoliths is assayed. Two-dimensional mapping provides literally a more complete picture of the dynamics of elemental incorporation. Whereas 2D mapping is possible with other microbeam techniques (electron microprobe, μ PIXE), we have been successful at mapping trace elements at lower concentrations than by other methods. Thus, this method represents an advance in the general area of spatial analysis of otolith chemistry.

Our method has much to contribute to the rapidly developing use of elemental fingerprinting to identify lifetime habitat use by fishes.¹ Importantly, the visualizations we obtain from 2D maps show convincingly the heterogeneity of elemental distributions in otoliths, providing insights (e.g. habitat signatures) and stimulating new questions (how elements are differentially incorporated into otoliths, and how they are retained). It also illustrates the potential problems of relying on point or transect measurements of elements in otoliths; the 2D maps show that different parts of otoliths

may accumulate elements at different rates (e.g. Figure 2(E)), so that a line transect collected on a given otolith growth axis may not truly reflect the history of elemental exposure.

COMMENTS AND RECOMMENDATIONS

Although it is unlikely that this synchrotron-based method, which requires high-intensity sources of x-rays, will ever be widespread enough to accommodate the potentially thousands of applications in fisheries, the ability to screen and detect multiple elements at low concentrations simultaneously, and at the fine scale necessary in otoliths, lends the method to further directed pilot studies. We do, however, anticipate that sample collection will improve with more powerful detectors and refinements to the methods, so that data collection times will drop. We would encourage others who have access to synchrotron-source XRF facilities with microbeam analytic capability to explore the use of high-capacity data collectors.

Furthermore, this work should stimulate research and development to improve other nondestructive microanalytic methods, both in terms of resolution, rapid data collection, and other difficult-to-measure analytes (e.g. stable isotopes). We believe that future results will provide new and novel information in the realm of aquatic monitoring of environmental conditions as well as surprising insights in fish life history.

Acknowledgements

We thank the Hudson River Foundation, the National Science Foundation (grant No. DEB 0238121), and the Great Lakes Protection Fund for support of this effort. The synchrotron x-ray fluorescence work was conducted at the Cornell High Energy Synchrotron Source (CHESS), which is supported by the National Science Foundation and the National Institutes of Health/National Institute of General Medical Sciences under grant award DMR 0225180. We thank E. Fontes of CHESS for his help with the early stages of this study and L. Vincze for a copy of his Monte Carlo simulation program. P. Thompson, D. Gefell, L. Westin, and J. Hasse assisted with fish collection and discussion of results. Comments by S. Gruner, P. Hanson, C. Jones, D. Swaney, and anonymous reviewers improved the manuscript.

REFERENCES

1. Campana SE, Thorrold SR. *Can. J. Fish. Aquat. Sci.* 2001; **58**: 30.
2. Campana SE. *Mar. Ecol. Prog. Ser.* 1999; **188**: 263.
3. Secor DH, Henderson-Arzapalo A, Piccoli PM. *J. Exp. Mar. Biol. Ecol.* 1995; **192**: 15.
4. Tzeng WN, Severin KP, Wickström H. *Mar. Ecol. Prog. Ser.* 1997; **149**: 73.
5. Arai T, Kotake A, Ohji M, Miyazaki N, Tsukamoto K. *Fish. Sci.* 2003; **69**: 813.
6. Limburg KE, Elfman M, Kristiansson P, Malmkvist K, Pallon J. *AIP Conf. Proc.* 2003; **680**: 339.
7. Milton DA, Chenery SR. *J. Fish Biol.* 1998; **53**: 785.
8. Proctor CH, Thresher RE. *Mar. Biol.* 1998; **131**: 681.
9. Rooker JR, Zdanowicz VS, Secor DH. *Mar. Biol.* 2001; **139**: 35.
10. Kumakhov MA. *X-Ray Spectrom.* 2000; **29**: 343.
11. Balaic DX, Nugent KA, Barnea Z, Garrett R, Wilkins SW. *J. Synchrotron Radiat.* 1995; **2**: 296.
12. Bilderback DH, Hoffman SA, Thiel DJ. *Science* 1994; **263**: 201.
13. Bilderback DH, Huang R, Kazimirov A, Kriksunov IA, Limburg K, Fontes E. *Adv. X-ray Anal.* 2003; **46**: 320.
14. Huang R, Bilderback DH. *J. Synchrotron Radiat.* 2006; **13**: 74.

15. Vincze L, Janssens K, Adams F, Rivers ML, Jones KW. *Spectrochim. Acta* 1995; **50B**: 127.
16. Ojaveer E, Lehtonen H. *Ambio* 2001; **30**: 217.
17. Andersson PS, Wasserberg GJ, Ingri J. *Earth Planet. Sci. Lett.* 1992; **113**: 459.
18. Andersson PS, Wasserberg GJ, Ingri J, Stordal MC. *Earth Planet. Sci. Lett.* 1994; **125**: 195.
19. Winterhalter B, Flodén T, Ignatius H, Axberg S, Niemistö L. In *The Baltic Sea*, Voipio A (ed). Elsevier Scientific: Amsterdam, 1981; 1.
20. Limburg KE, Landergren P, Westin L, Elfman M, Kristiansson P. *J. Fish Biol.* 2001; **59**: 682.
21. Halden NM, Mejia SR, Babaluk JA, Reist JD, Kristoferson AH, Campbell JL, Teesdale WJ. *Fish. Res.* 2000; **46**: 289.
22. Bigelow HB, Schroeder WC. *Fishes of the Gulf of Maine*. U.S. Government Printing Office: Washington, DC, 1953.
23. Owens RW, O'Gorman R, Mills EL, Rudstam LG, Hasse JJ, Kulik BH, MacNeill DB. *J. Great Lakes Res.* 1998; **24**: 723.
24. Limburg KE, Blackburn I, Schmidt R, Lake T, Hasse J, Elfman M, Kristiansson P. *Bull. Fr. Pêche Piscic.* 2001; **362/363**: 931.
25. Limburg KE, Siegel DI. *Northeastern Geol. Environ. Sci.* 2006; **28**: 254.
26. Effler SW (ed). *Limnological and Engineering Analysis of a Polluted Urban Lake: Prelude to Environmental Management of Onondaga Lake, New York*. Springer: New York, 1996.
27. Geffen AJ, Pearce NJG, Perkins WT. *Mar. Ecol. Prog. Ser.* 1998; **165**: 235.
28. Thresher RE. *Fish. Res.* 1999; **43**: 165.
29. Gatlin DM III, Wilson RP. *J. Nutr.* 1984; **114**: 627.
30. Cowey CB, Mackie AM, Bell JG (eds). *Nutrition and Feeding in Fish*. Academic Press: New York, 1985.
31. Skorupa JS. In *Environmental Chemistry of Selenium*, Frankenberger WT Jr, Engberg RA (eds). Marcel Dekker: New York, 1998; 315.
32. Lemly AD. *Selenium Assessment in Aquatic Ecosystems*. Springer: New York, 2002.
33. Pelletier E. *Mar. Environ. Res.* 1986; **18**: 111.
34. Siegel BZ, Siegel SM, Correa T, Dagan C, Galvez G, Leeloy L, Padua A, Yaeger E. *Arch. Environ. Contam. Toxicol.* 1991; **20**: 241.
35. Tsukamoto K, Nakai I, Tesch W-V. *Nature* 1998; **396**: 635.
36. Elsdon TS, Gillanders BM. *Rev. Fish Biol. Fish.* 2003; **13**: 219.
37. Thorrold SR, Jones CM, Campana SE, McLaren JW, Lam JWH. *Limnol. Oceanogr.* 1998; **43**: 1826.
38. Campana SE. In *Stock Identification Methods*, Cadrin SX, Friedland KD, Waldman JR (eds). Elsevier: Amsterdam, 2005; 227.
39. Gillanders BM. *Mar. Ecol. Prog. Ser.* 2002; **240**: 215.